ACTA METALLURGICA SLOVACA
2022, VOL. 28, NO. 3, 127-132

RESEARCH PAPER

VANADIUM ALLOYING IN S355 STRUCTURAL STEEL: EFFECT ON RESIDUAL AUSTENITE FORMATION IN WELDED JOINTS HEAT AFFECTED ZONE

Giulia Stornelli[1], Matteo Gaggiotti[2], Daniele Mirabile Gattia[3], Rolf Schmidt[4], Mirko Sgambetterra[5], Anastasiya Tselikova[4], Guido Zucca[5], Andrea Di Schino[2]

[1] Università di Roma Tor Vergata, Dipartimento di Ingegneria Industriale, Roma, Italy
[2] Università degli Studi di Perugia, Dipartimento di Ingegneria, Perugia, Italy
[3] Dipartimento Sostenibilità dei Sistemi Produttivi e Territoriali, ENEA - CR Casaccia, Roma, Italy
[4] Metals AG, Zug, Switzerland
[5]Aeronautica Militare – Divisione Aerea di Sperimentazione Aeronautica e Spaziale, Via Pratica di Mare 45, 00040 Pomezia RM, Italy

*Corresponding author: giulia.stornelli@students.uniroma2.eu, Dipartimento di Ingegneria Industriale, Roma, Italy

Received: 16.06.2022
Accepted: 01.07.2022

ABSTRACT

The inter-critical heat affected zone (ICHAZ) appears to be one of the most brittle sections in the welding of high-strength micro-alloy steels (HSLA). Following multiple heating cycles in the temperature range between Ac_1 and Ac_3, the ICHAZ undergoes a strong loss of toughness and fatigue resistance, mainly caused by the formation of martensite-austenite constituent (MA). The presence of micro-alloying elements in HSLA steels induces variations in the formation of some microstructural constituents, more or less beneficial, which allow to improve the mechanical performance of a welded joint. The behavior in the inter-critical region of a S355 grade steel with 0.1wt% V addition is reported in this paper. Five double-pass welding thermal cycles were simulated using a dilatometer, with the maximum temperature of the secondary peak in the inter-critical area, in the range between 720 °C and 790 °C. The residual austenite dependence on inter-critical temperature is analyzed and related to the hardness behavior.

Keywords: micro-alloying, vanadium, residual austenite

INTRODUCTION

The development of high strength materials for oil and gas and energy application has been driven in last times by customer requests to combine high tensile properties, impact resistance and good weldability on industrial scale at prices responding to market requests [1-5]. A comparable figure is met in different market sectors of structural steels (for example offshore metallic structures or ships, with broadly similar aims). In such cases anyway, the target of strength/toughness combination is largely affected by the specific design [6]. Vanadium, following its peculiar thermodynamic and kinetic attitude to form very fine precipitates in form of VC or VCN, played a key role in the design of microstructures and processes of modern HSLA steels [7-9].

The above reported materials for sure made possible the efficient design of constructions also facing with market requirements [10-13]. As far as concerns pipelines for long distance gas transportation, for example, the increase in the available strength level taking place during the last decades lead to benefits which can be estimated in billion-dollar range [14].

The effect of micro-alloying on the microstructure features and on the mechanical properties of a girth weld is a very hot topic since it interrelates a huge quantity of mechanisms strictly connected and strongly affected by the steel chemical composition and the welding conditions [15-17].

Despite the micro-alloying relevance in the metallurgical design of HSLA for gas transportation, general trend reporting a decrease in the properties of girth welded joints is found by many authors in the open literature [18]. This is why micro-alloying strategy has been often limited in the last years by many steel makers.

The proper equilibrium between strength and fracture toughness in high strength low alloyed steels is strictly related to the thermal cycles reported by the materials during the welding process: as a matter of fact such thermal cycle is the main responsible for the toughness properties loss specifically in the heat affected zone (HAZ).

Many papers report that the most critical zone (showing the lowest impact resistance) is expected to be found in the grain coarsened heat affected zone (GC HAZ) [19-21]. Such region of the welded joint is the one immediately neighbouring the weld fusion line. During the welding process, the peak temperature to which the materials is subjected in the GC HAZ faces to the melting point. Such peak temperatures are then followed by very rapid cooling. Facing such high temperatures implies a significant austenite grain size coarsening [22]. The presence of large austenitic grains together with rapid cooling experienced by the material, promotes the nucleation of brittle components. Such components are constituted by ferrite-bainite microstructures together with fine micro-constituents [23].

In recent years, it has been shown that the inter-critically reheated grained HAZ (IC GC HAZ) is the welded joint region mostly affected by the mechanical property loss [24]. One of the suggested metallurgical mechanisms which has been proposed to explain such behaviour is that during the inter-critical thermal cycle, partial transformation to austenite occurs. The above consideration is valid especially for steels

showing the presence of austenite stabilizers, such as carbon or manganese. Such phenomena are usually favoured by the presence of segregation in the initial microstructure, mainly related to the manufacturing process [25]. During the rapid cooling step of the welding process these carbon rich material portions are subjected to phase transformation into pearlite/bainite or residual austenite (RA). The presence of residual austenite and the main phase choose depends on the steel hardenability, hence on the steel chemical composition and the alloying strategy adopted by the steel maker [26]. The presence of RA phase is generally considered as the main cause responsible for impact resistance loss in HAZ.

Nonetheless, the issue is much more complicated since some authors reported that the impact resistance loss is not just and solely related to the presence of RA micro-constituent. A clear role in terms of RA distribution and morphology in relation to the main matrix microstructure is found.

A strategy based on Nb addition is sometimes followed in the design of high strength steels with acceptable toughness behaviour.

It has been shown that niobium affects the HAZ by negative consequences [27]. Is also been reported that such effects are strongly dependent on the adopted heat input [28].

On the contrary, the effects of vanadium addition on the toughness of the IC GC HAZ and on the formation of M-A phase within the IC GC HAZ are not up-today fully clear and understood.

Some authors reported that vanadium has a negative effect on the impact resistance of the IC GC HAZ. This behaviour is manly related to vanadium ability to promote the formation of the potentially brittle M-A phase [29]. However, other researchers showed that the addition of vanadium to low carbon steels reduced the size and area fraction of M-A phase and improved IC GC HAZ toughness [30].

In this paper, the effect of Vanadium addition to an S355 for structural application (EN10025-2) steel during heat treatments reproducing the HAZ of a welded joint is reported, in terms of M-A formation.

MATERIAL AND METHODS

A steel with chemical composition as reported in **Table 1** was manufactured by Vacuum Induction Melting (VIM) plant in the form of 80 kg ingot and then hot rolled down to 16 mm thickness. The hot rolled microstructure after 2% Nital etching is reported in **Figure 1**.

Table 1 Nominal chemical composition of considered steel (wt%)

Element	Wt, %
C	0,16
Mn	1.45
V	0,10
Fe	To balance

Heat treatments were designed with the aim to reproduce different microstructures corresponding to different positions in a welded joint HAZ. In particular a double pass welding process has been simulated with second pass peak temperatures ranging from 720 °C to 790 °C. In order to investigate the presence of retained austenite (RA) and to define the most suitable methodology to assess the RA presence in the considered steel after the heat treatment as reported above, three different methods have been applied: X-Ray Diffraction (XRD), Electron Backscattered Diffraction (EBSD), and selective Le Perà etching. XRD analysis was carried out using a Smartlab Rigaku diffractometer equipped with Cu kα source radiation and a D/teX Ultra 250 SL detector, operated at 40 kV and 30 mA in continuous mode in the angular range 30-110 2theta. The automated sample alignment routine has been used. Rietveld analysis has been performed on diffracted data in order to ascertain weight percent phase fractions. EBSD measurements were performed with the aim to detect the presence and position of retained austenite islands, by means of a field emission gun scanning electron microscope (FEG-SEM) (Ultra-Plus Carl-Zeiss- Oberkochen Germany) equipped with an EBSD detector (C Nano Oxford Instruments United Kingdom), using a 0.1 µm scanning step size. Retained austenite was revealed by building up phase maps, taking into account both face-centered cube (fcc) and body-centered cube (bcc) phases: automatic image analysis of such maps allowed us to determine retained austenite volume fraction.

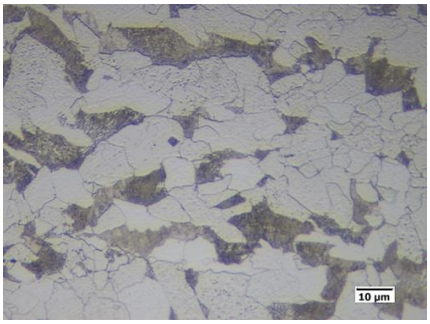

Fig. 1 Hot rolled material (2% Nital etching)

Starting from the hot rolled material, cylindrical Specimens (10 mm in length, 4 mm in diameter) were machined to be heat treated in controlled conditions by means of a dilatometer. Heat treatments cycles as reported in **Figure 2**.

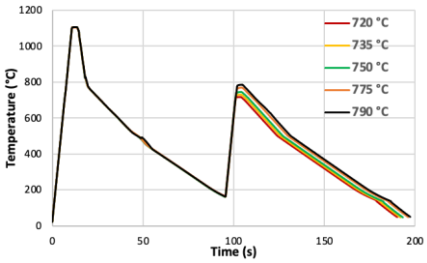

Fig. 2 Experimental thermal profiles as acquired by thermocouples

Indeed, as regards the selective etching, the LePerà solution (1g H2S2O5 + 100ml H2O + 4g C6H3N3O7 + 100ml C2H5OH) for about 60-90 seconds was used. The microstructure was then analyzed using an optical microscope (OM) (Eclipse LV150 NL, Nikon, Tokyo, Japan) and an image analysis, to determine the RA percentage, was performed using dedicated software (AlexaSoft, X-Plus, serial number: 6308919690486393, Florence, Italy). The procedures was performed on low magnification image and on three different fields, the RA % reported will be refers to the average of three values. Vickers hardness tests were made by means of a HV50 (Remet, Bologna, Italy) instrument by using a load of 10 kg. Three hardness tests were made on each sample.

RESULTS

Microstructures, as obtained after thermal cycles, are shown in **Figure 3**. Results show that, moving from 790 °C (as second

peak temperature) down to 720 °C, microstructure moves from ferrite-pearlite to bainite, as expected.

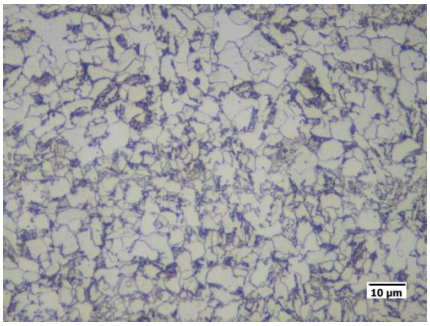

Peak temperature=790 °C

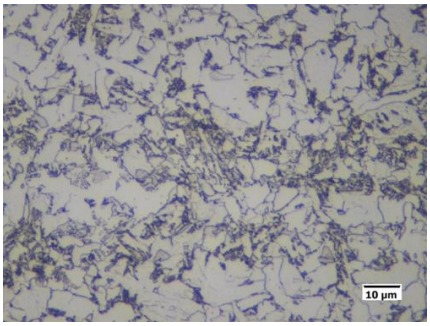

Peak temperature=775 °C

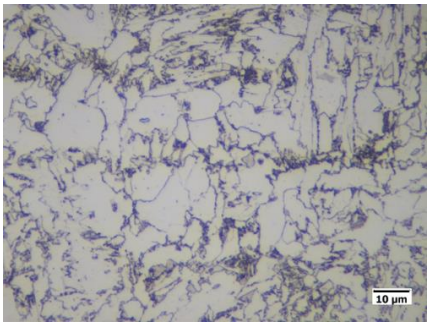

Peak temperature=750 °C

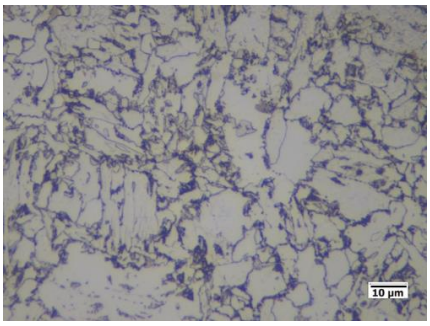

Peak temperature=735 °C

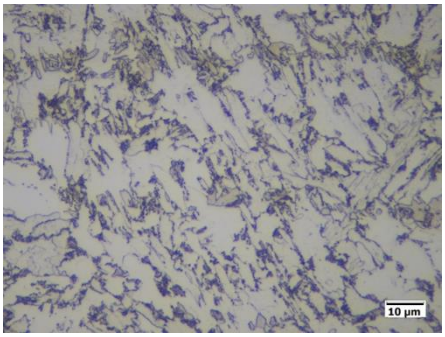

Peak temperature=720 °C

Fig. 3 Obtained microstructure as a function of second peak temperature (2% Nital etching)

In order to evaluate the RA content on the above considered specimens, XRD patterns have been acquired. Results, reported in **Figure 4**, are not able to discriminate between the different conditions: in particular the detected residual austenite is very low, at the limit of the acceptability threshold of the technique, generally below 1 wt.%. Results therefore show that X-Ray technique is not suitable for RA determination in HAZ in the considered set of samples.

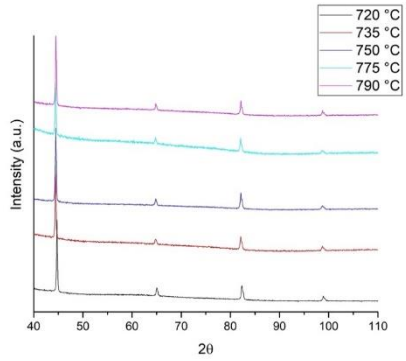

Fig. 4 X-Ray diffraction data of the considered materials

Phase maps as obtained by EBSD technique on the considered materials are reported in **Figure 5**. Staring from pictures reported in **Figure 5**, the RA content (red zones) has been evaluated as a function of the peak temperature.

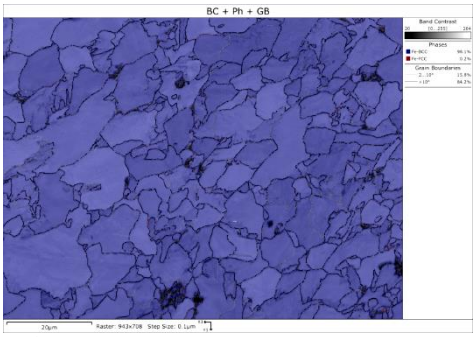

Peak temperature=790 °C

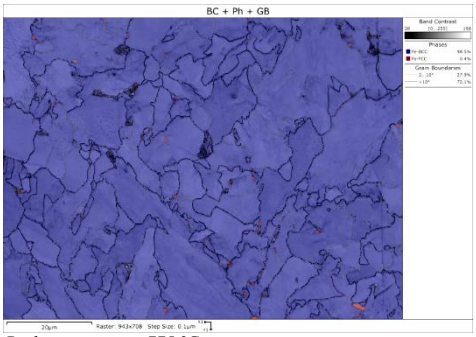

Peak temperature=775 °C

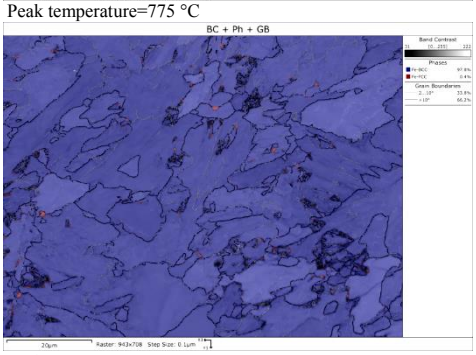

Peak temperature=750 °C

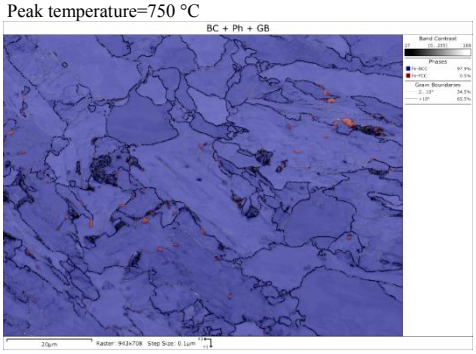

Peak temperature=735 °C

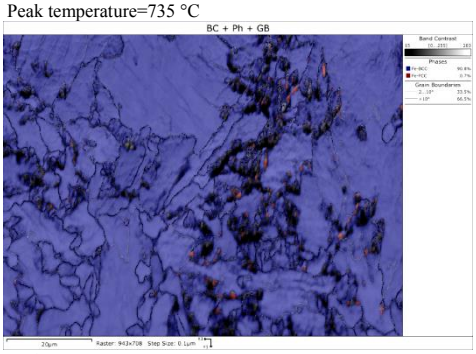

Peak temperature=720 °C

Fig. 5 Phase maps as obtained by EBSD technique on the considered materials

Results, reported in **Table 2**, show very low RA contents, confirming that they are well below the XRD threshold.
RA content has also been evaluated by quantitative optical microscopy metallography after Le Perà selective etching. The relevant microstructures with RA islands highlighted in red are reported in **Figure 6**.

Table 2 RA dependence on peak temperature as obtained by EBSD

Peak temperature (°C)	RA, %
790	0.7
775	0.2
750	0.3
735	0.2
720	0.4

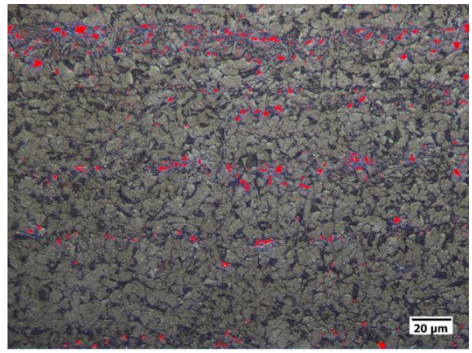

Peak temperature=790 °C

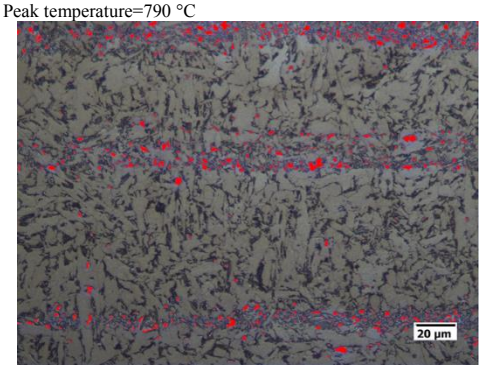

Peak temperature=775 °C

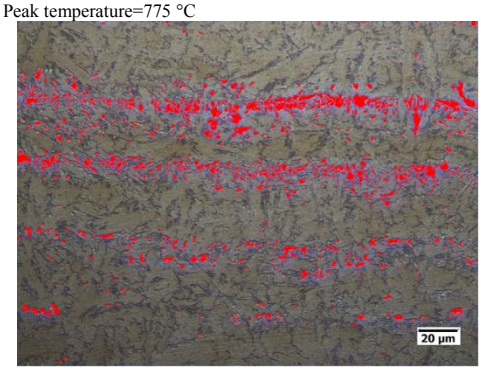

Peak temperature=750 °C

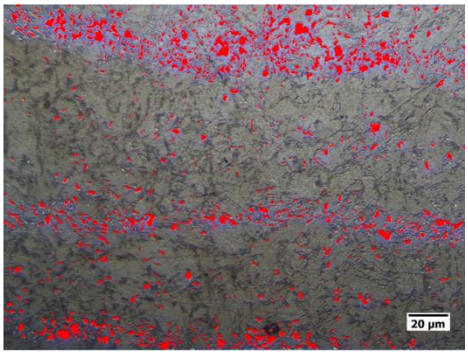

Peak temperature=735 °C

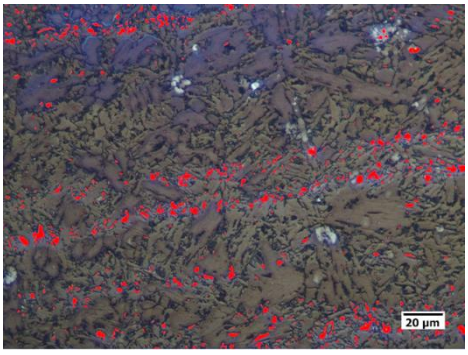

Peak temperature=720 °C

Fig. 6 Microstructures of the considered specimens after Le Perà etching. Red zones: RA phase

Results, reported in **Table 3**, show that RA values as measured by this technique are higher than those obtained by EBSD, as expected.

Table 2 RA dependence on peak temperature as obtained by EBSD

Peak temperature (°C)	RA, %
790	1.5
775	2.0
750	4.5
735	4.6
720	3.3

It has to be noted that results coming from EBSD are to be considered not to be affected by external factors (such etching) which could artificially enlarge the small RA regions. On the other hand, EBSD is not so statistically significant as optical microscopy measurement, following the smallest analysed areas. This is why both the methods need to be considered and results are to be considered as complementary.

RA values as obtained by EBSD and selective etching are compared in **Figure 7**, showing similar trend. Results reported in **Figure 8** show that the same trend is followed by hardness as measured on the same specimens.

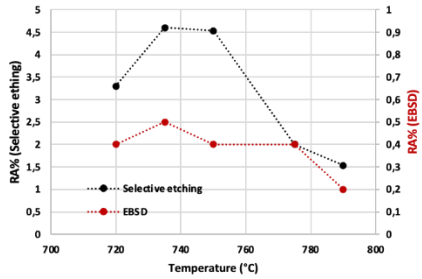

Fig. 7 RA dependence on peak temperature (comparison between EBSD and light microscopy)

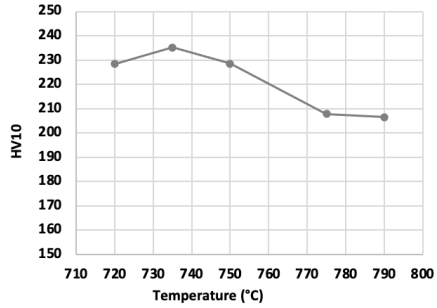

Fig. 8 Hardness dependence on peak temperature.

Results therefore suggest a direct influence of RA content, also at the very low measured level, in defining the mechanical properties.

CONCLUSIONS

The behavior in the inter-critical region of a S355 grade steel with 0.1wt% V addition is reported in this paper. Five double-pass welding thermal cycles were reproduced using a dilatometer, with the maximum temperature of the secondary peak in the inter-critical area, in the range between 720 °C and 790 °C. The residual austenite dependence on inter-critical temperature is analyzed showing a direct relation with the hardness behavior.

REFERENCES

1. D.W. Kim, J. Yang: Materials Science and Engineering A, 843, 2022, 143151. https://doi.org/10.1016/j.msea.2022.143151.
2. S. Roy, N. Romualdi, M. Militzter, L. Collins: JOM, article in press. https://doi.org/10.1007/s11837-022-05280-6.
3. G .Stornelli, R. Montanari, C. Testani, L. Pilloni, G. Napoli, O. Di Pietro, A. Di Schino: Mat. Sci. Forum, 1016. 2021, 1302-1397. https://doi.org/110.4028/www.scientific.net/MSF.1016.1392.
4. G. Stornelli, M. Gaggiotti, S. Mancini, G. Napoli, C. Rocchi, C. Tirasso, A. Di Schino: Metals, 12, 2022, 200. https://doi.org/10.3390/met12020200.
5. G. Stornelli, A. Di Schino, S. Mancini, R. Montanari, C. Testani, A. Varone: Applied sciences, 11(22), 2021, 10598. https://doi.org/10.3390/app112210598.

6. J. Shimamura, D. Izumi, J.Kondo: International Journal of Offshore and Polare Engineering, 12, 2021, 613. https://dor.org/10.17736/ijope.2020.hj38.
7. J.K. Benz, S.W. Thompson: Materials Science abd Technology Connference and Exhibition, 1, 2017, 490. https://doi.org/10.7449/2017/MST_2017_490_498.
8. F. Fazeli, B.S. Amhirkhiz, C. Scott, M. Arafin, L. Collins: Materials Science and Engineering A, 720, 2018, 248. https://doi.org/10.1016/j.msea.2018.02.042.
9. T.N. Baker: Ironmaking and Steelmaking, 43, 2016, 264. https://doi.org/10.1179/1743281215Y.0000000063.
10. A. Di Schino: Metalurgija, 58, 2019, 347-351.
11. A. Di Schino, C. Testani: Metals, 10, 2020, 552. https://doi.org/ 10.3390/met10040552.
12. Y. Tian, M. Zhao: JOM, 74. 2022, 2409. https://doi.org/10.1007/s11837-022-05202-6.
13. L. Hiaogang: Journal of Materials Research and Technology, 11, 2021, 2092. https://doi.org/10.1016/j.jmrt.2021.02.049.
14. Y. Bay, R. Bhattacharyya, M.E. Mc Cormick, Elsevier Ocean Engineering Series, 3, 2001, 353. https://doi.org/10.1016/S1571-9952(01)80033-7.
15. M. Narimani, E. Hajjari, M. Ekendari, J.A. Szpunar: Journal of Materials Engineerng and Performance, 31, 2022, 3985. https://doi.org/10.1007/s11665-021-06454-0
16. R. Geng, J. Li, C. Shi, J. Zhi, B. Lu: Materials Science and Engineering A, 840, 2022, 142919. https://doi.org/10.1016/j.msea.2022.142919.
17. S. Shi, W. Wang, D. Ko: Metals, 2, 2022, 12. https://doi.org/ 10.3390/met12020242.
18. A. Lambert-Perlade, A.F. Gourges, J. Besson, T. Sturel, A. Pineau: Metallurgical and Materials Transactions A: Physical Metallurgy and Materials Science, 25, 2004, 1039. https://doi.org/10.1007/s11661-004-1007-6.
19. B.C. Kim, S. Lee, N.J. Kim, D.Y. Lee: Metallurgical Transactions A, 22, 1991, 139. https://doi.org/10.1007/BF03350956.
20. Y. Shi, Z. Han: Journal of Mateials Processing Technology, 207, 2008, 30. https://doi.org/10.1016/j.jmatprotec.2007.12.049.
21. K. Prasad, D.K. Dwivedi: International Journal of Advanced Manufacturing Technology, 35, 2008, 457. https://doi.org/10.1007/s00170-006-0855-1.
22. T. Kvackaj, J. Bidulskà, R. Bidulsky: Materials, 14, 2021, 1988. https://doi.org/10.3390/ma14081988.
23. P. Prislupcak, T. Kvackaj, J. Bidulska, P. Zahumensky, V. Homolova, P. Zimovcak: Acta Metallurgica Slovaca, 27, 2021, 207-209. https://doi.org/10.36547/ams.27.4.1306.
24. G. Napoli, A. Di Schino, M. Paura, T. Vela: Metalurgija, 57, 2018, 111-113.
25. C. Ouchi: ISIJ International, 41, 2001, 542. https://doi.org/10.2355/isijinternational.41.542.
26. G. Spanos, R.W. Fonda, R.A. Vandermeer, A. Matuszeski: Metallurgical and Materials Transactions A: Physical Metallurgy and Materials Science, 26, 1995, 3277. https://doi.org/10.1007/BF02669455.
27. A. Di Schino: Metalurgija, 56, 2017, 349-352.
28. S. Lee, B.C. Kim, D. Kwon: Metallurgical Transactions A, 23, 1992, 2803. https://doi.org/10.1007/BF02651759.
29. Y. Li, D.N. Crowther, M.G.W. Green, P.S. Mitchell, T.N. Baker, ISIJ International, 41, 2001, 46. https://doi.org/10.2355/isijinternational.41.46.
30. S. Mitchell, P. H. M. Hart, W. B. Morrison: Proc. Microalloying 95', ISS, Warrendale, PA, (1995), 149.